

Satellite-Based Food Market Detection for Micronutrient Deficiency Prediction

Nikhil Behari,¹ Elizabeth Bondi,¹ Christopher D. Golden,²
Hervet J. Randriamady,³ Milind Tambe¹

¹ Center for Research on Computation and Society, Harvard University
² Harvard T.H. Chan School of Public Health

³ Madagascar Health and Environmental Research (MAHERY)
nikhilbehari@college.harvard.edu, ebondi@g.harvard.edu

Abstract

“Hidden Hunger,” or micronutrient deficiency (MND), is a nutritional disorder caused by a lack of essential vitamin and mineral intake, often leading to severe physical and mental developmental impairment. MND is highly prevalent worldwide, particularly in South Asia, South America, and sub-Saharan Africa, affecting an estimated 2 billion people. While intervention programs exist to treat MND, identifying susceptible regions at a large scale may require time-intensive and costly blood draws and/or household surveys. Public health research in MND indicates that food markets are often correlated with improved dietary diversity, a proxy for MND prediction. However, data on market locations is limited. We propose an approach to automatically detect regional food markets from publicly available geographic infrastructure data and satellite imagery, which may be used towards developing a cost-effective, noninvasive MND prediction model.

Introduction

An estimated 2 billion people worldwide are impacted by micronutrient deficiency (MND), a nutritional disorder caused by a lack of essential vitamins and minerals. Common forms of nutrient deficiencies include Vitamin A deficiency, affecting 190 million preschool-age children, and iron deficiency, affecting more than 30% of the world’s population (WHO 2011). MND has severe impacts on physical and mental development in children and infants, potentially leading to a weakened immune system, blindness, and/or birth deformities. It is often described as “Hidden Hunger” due to the lack of early physical indicators unlike other common forms of undernutrition, such as wasting (Muthayya et al. 2013).

Intervention programs such as food fortification and dietary diversification are effective for treating MND, particularly for pregnant women and children (UNICEF 2017; Horwitz et al. 1998). However, because MND is difficult to detect from physical appearance alone, blood draws and/or household surveys may be required for identifying susceptible regions and targeting intervention programs. These blood draws and household surveys may be time-intensive and costly, making large-scale efforts for MND prediction inaccessible.

Copyright © 2021, Association for the Advancement of Artificial Intelligence (www.aaai.org). All rights reserved.

Public health research in MND prevention points to several nutritional, environmental, and socioeconomic factors related to MND. In particular, evidence suggests that better access to markets is correlated with improved dietary diversity (Hirvonen et al. 2017; Koppmair, Kassie, and Qaim 2017), a characteristic often used as a proxy for MND (Kennedy et al. 2007; Arimond and Ruel 2004). Towards developing an automatic MND prediction methodology, we hypothesize that both publicly available geographic infrastructure data and satellite imagery can be used to determine market access. We focus this research on Madagascar, which has one of the highest rates of chronic malnutrition and MND worldwide, using survey data from four distinct regions as ground truth data of market characteristics. This approach enables regional analysis for market access, which may serve as an efficient, cost-effective, and noninvasive indicator of MND.

Related Work

Satellite-based remote sensing has become a popular approach in public health research for identifying correlates of diseases such as malaria and malnutrition. (Heft-Neal et al. 2018) find that satellite-based data products measuring particulate matter may be used to determine infant mortality rates. (Johnson, Jacob, and Brown 2013) use satellite imagery to show a negative correlation between forest cover loss and dietary diversity in Malawi. Land cover classification, typically produced from satellite image segmentation, is a common product used in modelling malaria risk and transmission (Stefani et al. 2013).

There is also a large body of work aimed towards developing geospatial data products in general, which may be used for public health efforts. Volunteered geographic information (VGI) projects, such as OpenStreetMap (OSM) (OpenStreetMap contributors 2017), aim to map and record georeferenced data of the Earth. Several studies aim to identify regional economic activity from satellite imagery, including through nighttime light sensing (Doll, Muller, and Morley 2006; Bennett and Smith 2017). Image segmentation is also frequently used to derive data products from satellite imagery, such as land cover, crop production, or infrastructure. In particular, U-Net segmentation architecture is a popular approach for satellite-based building and road segmentation (Iglovikov, Mushinskiy, and Osin 2017; Zhang, Liu,

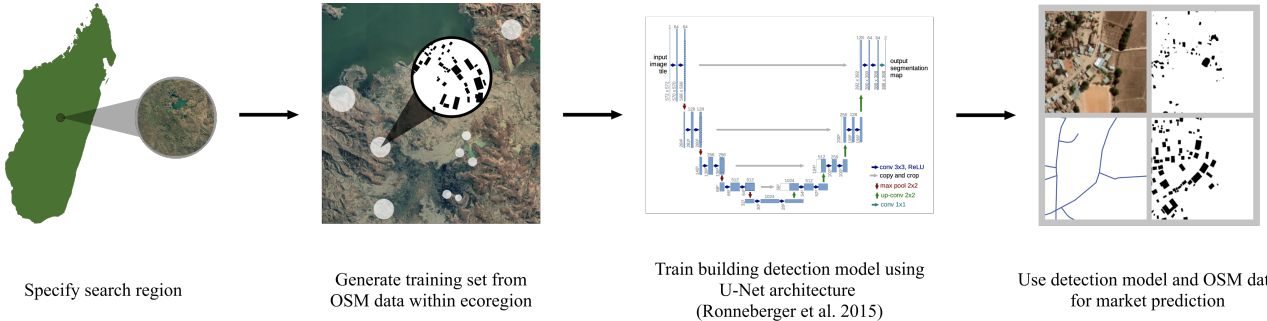


Figure 1: Methodology for region-specific training set generation and building detection model training.

and Wang 2018).

There are some related works that attempt to determine market location and market access. (Weiss et al. 2018) develop a worldwide “travel time to cities” map to determine the worldwide inequality in urban center accessibility, using OSM and Google Maps to determine specific times of travel using various modes of transportation. This research improves upon previous efforts to quantify travel time to markets that use Euclidean or network distance, but only determines travel times to large population centers. (Baragwanath et al. 2019) aim to detect urban markets using nighttime light and daytime landcover data products, applied to urban centers in India. (Ackermann et al. 2020) use satellite imagery to quantify infrastructure features as an indicator of economic development. Similarly, (Oshri et al. 2018) aim to quantify infrastructure quality using 10m and 30m resolution satellite imagery, which may lack granularity for detection of smaller markets. Instead, we propose to use region-specific models to determine building counts and road access, which may then be used as predictors of markets.

Market Data

To better understand the characteristics of regional markets, we referenced focus group data from four distinct ecological regions in Madagascar to develop a market detection model. These four ecological regions were used to represent the large degree of ecological diversity in the country, which results in highly variant terrain appearances in satellite imagery. We broadly classify these regions as 1) higher elevation central plateau, 2) high rainfall east coast, 3) seasonally dry west coast, and 4) arid south and southwest. Respondents from 24 locations across these four regions provided a description of their nearest food markets with associated walking times. These responses were used to identify regional markets in order to determine basic satellite-based predictors.

Methodology

We develop an automatic pipeline for market detection by first identifying features of markets visible from satellite imagery based on the regional survey data. We determine reasonable classification thresholds for these identified features, then use these thresholds to determine the efficacy of

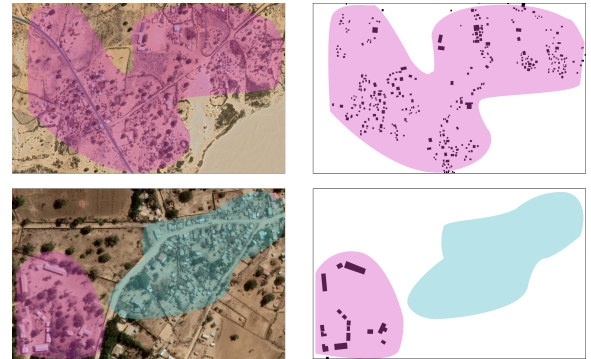


Figure 2: Populated (top) vs. sparse (bottom) OSM data. Complete data is highlighted in pink, while missing data is highlighted in blue.

VGI resources, such as OSM, in market detection. Finally, we test a satellite image-based segmentation model using OSM data as model training inputs, towards improving the detection accuracy of identified classification predictors.

Predicting Market Presence

Comparing the survey data responses with satellite imagery, we inferred that the number of buildings within town clusters and proximity to highways may be used as predictors of market presence in Madagascar. Using these features as market prediction inputs, we determined classification thresholds by first assigning central coordinates to each known market location, identified from the survey data responses. We then selected the minimum required search radius, building counts, and road counts necessary to correctly identify all survey-identified markets from satellite imagery. This resulted in a classification threshold with a search radius of 0.5km, where locations with more than 20 buildings and one highway within that radius would be classified as likely containing markets. In order to apply these thresholds in an automatic market detection pipeline, we must first accurately determine road and building presence within a region.

OSM-Based Segmentation

We first evaluate the accuracy of market prediction using OSM data alone to determine the number of buildings and

highways within a specified region. The results from this initial market classification approach indicated that OSM data alone were not sufficient for market detection. In particular, while data on roads and highways were accurate in comparison to satellite imagery, OSM data on buildings in several areas was sparse or entirely missing, resulting in several unmarked building clusters (Figure 2). As a result, roughly half of the known set of markets were not identified by the OSM data-based prediction model. These inaccuracies motivated the development of a satellite-based building detection model to identify potential markets in areas with sparse geographic data.

Satellite-Based Segmentation

In order to detect these missing buildings in satellite imagery, we tested the use of semantic segmentation (Figure 1).

Gathering Training Data To automatically generate training data for the building segmentation models, we sampled locations across the four classified ecoregions in Madagascar corresponding to the locations of known markets. For each ecoregion, we automatically identified the closest densely clustered OSM building labels to the known market locations. Densely clustered OSM label regions, determined by the number of building labels per square kilometer, were prioritized in this search over sparse labels in order to avoid extreme false negative presence in the training data. The regions containing the identified building labels were then saved as image masks, and the corresponding satellite images were saved to the image training set.

To save the satellite images, we used the Google Maps Static API. This approach allows for open access, rapid, batch downloads of high resolution imagery. Images may be requested through API calls made through URL requests, allowing for image parameter specification including image center (a latitude/longitude pair), zoom level, and image format. The resulting image may then be downloaded for use in the image segmentation pipeline. While these requests are not free, there is a \$200 monthly Google Maps Platform credit available that was sufficient for generating our full dataset. In total we generated four datasets, each corresponding to a classified ecoregion, with each data set containing roughly 100-200 training images and at least 500 corresponding OSM building labels across all images. Each individual image was 600x600 pixels, with a 0.46 meter resolution.

U-Net Model Training Using the automatically generated training data, we then generated a training and testing split for each region to determine the efficacy of the respective building detection models. We used a U-Net convolution network (Ronneberger, Fischer, and Brox 2015) with a ResNet-34 encoder pretrained on ImageNet (Deng et al. 2009). The U-Net architecture, originally developed for biomedical image segmentation, is commonly used for satellite image segmentation, and is particularly useful for training on smaller training sets such as the sparse OSM building label data (Ronneberger, Fischer, and Brox 2015).

Ecoregion	Precision	Recall
Central Plateau	0.4455	0.4108
Southeast	0.6503	0.4197
West Coast	0.6869	0.3328
Southwest	0.5915	0.2436

Table 1: Satellite image building segmentation performance on testing subset, grouped by ecoregion.

OSM	OSM + Satellite Detection
0.48	0.86

Table 2: Precision comparison of market prediction. The percentage of known markets identified from OSM data alone compared to OSM data augmented with satellite-based building detection.

The satellite image training set was augmented with random flips, rotations, and resizes. Binary cross entropy was used for the loss function, and we used the Adam optimizer (Kingma and Ba 2014) with a learning rate of 1e-2. The model was trained using a batch size of 16.

Results

Precision and recall results for the satellite image-based building segmentation model are shown in Table 1. The comparison of known markets identified using only OSM data with OSM data augmented with the satellite-based segmentation is shown in Table 2. Examples of model predictions on satellite images compared to OSM data across the four regions are shown in Figure 3. We found, as expected, that the segmentation performance was dependent on the terrain and region types. For example, humid forest regions contain significantly more tree cover than spiny thickets regions, potentially leading to a greater contrast between building and non-building appearance. Alternatively, some regions, such as the West Coast, had significantly less OSM data within the region to train on, likely reducing the accuracy of the building detection model in the training results. Regardless, the model performs well enough to identify approximate building locations, with a relatively high precision that avoids false positives for market detection.

A comparison of results indicates that the number of known markets identified is significantly improved when including the building detection model as an input. Upon manual inspection, OSM data were entirely missing within several identified market regions, while the satellite-based building detection model was effective in locating these clusters of buildings.

Discussion

It is important to note that OSM is not the only source for georeferenced infrastructure and mapping data. Google Maps, for example, is an alternative source for georeferenced data that may include more complete data than OSM

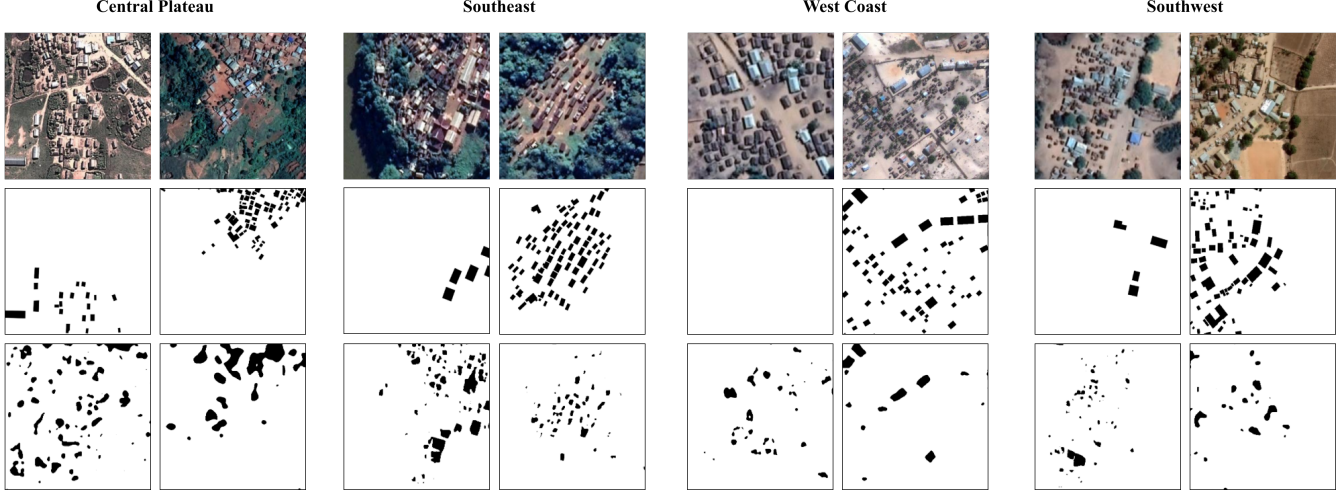


Figure 3: Semantic building segmentation results for each ecoregion. (Top) Satellite image (Center) OSM labels (Bottom) Model predictions; (Left) Sparse OSM data, (Right) Complete OSM data.

in some areas. However, these data can be harder to access, and still sparse for many regions. Our methodology may be used to augment existing geographic mapping data towards improving accuracy of market detection. This approach is flexible, in that a similar methodology may be applied to areas worldwide given regional context.

Using the region-specific training data generation process, we saw good performance for the satellite image-based building segmentation models. Training set labels were derived from building data within a close proximity of areas of interest, primarily within one ecoregion. However, while we distinguish between ecoregions in training region-specific models in this work, we believe that the proposed methodology is applicable for any type of localized region with approximately the same infrastructure and geography.

While we believe this methodology may be generalizable, we also identify several areas for future work. First, we envision that travel time to one of the markets we identify may provide a better metric for market access in predicting MND. (Weiss et al. 2018), for example, created geographic travel time maps to quantify market access worldwide, defining markets as population centers of at least 50,000 inhabitants. We believe this approach could complement our proposed methodology to better predict MND. Furthermore, while we detect buildings to identify candidate locations for markets in this research, future research could focus on searching for markets directly. For example, based on focus group data and local insights, we learned that we could search for temporary stands, specific roofing materials, and/or semi-permanent structures rather than simply buildings, which may require more detailed training data. Finally, given the noted inaccuracies in OSM data, using these data for satellite image segmentation training inputs may introduce unwanted error from false negatives in building labels. To address this, we envision our methodology applied in an active learning pipeline to verify the accuracy of automatically generated training data. Even before making these advances, our pre-



Figure 4: Terrain differences in satellite imagery.

sented pipeline can be used to identify candidate market locations. We believe that we can use these locations, amongst other satellite-based predictors, to aid in efficiently identifying regions most susceptible to MND.

Additional Resources

The source code containing examples for implementation of satellite image download, model training, and testing can be found at <https://github.com/NikhilBehari/market-detection>.

Acknowledgments

This work was partially supported by the Army Research Office (MURI W911NF1810208). We are also grateful for the support from the United States Agency for International Development (grant AID-FFP-A-14-00008) implemented by Catholic Relief Services (CRS) in consortium with four local implementing partners in Madagascar. The views and opinions expressed in this paper are those of the

authors and not necessarily the views and opinions of the United States Agency for International Development.

References

- Ackermann, K.; Chernikov, A.; Anantharama, N.; Zaman, M.; and Raschky, P. A. 2020. Object Recognition for Economic Development from Daytime Satellite Imagery. *arXiv preprint arXiv:2009.05455*.
- Arimond, M.; and Ruel, M. T. 2004. Dietary diversity is associated with child nutritional status: evidence from 11 demographic and health surveys. *The Journal of nutrition* 134(10): 2579–2585.
- Baragwanath, K.; Goldblatt, R.; Hanson, G.; and Khandelwal, A. K. 2019. Detecting urban markets with satellite imagery: An application to India. *Journal of Urban Economics* 103:173.
- Bennett, M. M.; and Smith, L. C. 2017. Advances in using multitemporal night-time lights satellite imagery to detect, estimate, and monitor socioeconomic dynamics. *Remote Sensing of Environment* 192: 176–197.
- Deng, J.; Dong, W.; Socher, R.; Li, L.-J.; Li, K.; and Fei-Fei, L. 2009. Imagenet: A large-scale hierarchical image database. In *2009 IEEE conference on computer vision and pattern recognition*, 248–255. Ieee.
- Doll, C. N.; Muller, J.-P.; and Morley, J. G. 2006. Mapping regional economic activity from night-time light satellite imagery. *Ecological Economics* 57(1): 75–92.
- Heft-Neal, S.; Burney, J.; Bendavid, E.; and Burke, M. 2018. Robust relationship between air quality and infant mortality in Africa. *Nature* 559(7713): 254–258.
- Hirvonen, K.; Hoddinott, J.; Minten, B.; and Stifel, D. 2017. Children’s diets, nutrition knowledge, and access to markets. *World Development* 95: 303–315.
- Horwitz, A.; Kennedy, E. T.; Howson, C. P.; et al. 1998. *Prevention of micronutrient deficiencies: tools for policymakers and public health workers*. National Academies Press.
- Iglovikov, V.; Mushinskiy, S.; and Osin, V. 2017. Satellite imagery feature detection using deep convolutional neural network: A kaggle competition. *arXiv preprint arXiv:1706.06169*.
- Johnson, K. B.; Jacob, A.; and Brown, M. E. 2013. Forest cover associated with improved child health and nutrition: evidence from the Malawi Demographic and Health Survey and satellite data. *Global Health: Science and Practice* 1(2): 237–248.
- Kennedy, G. L.; Pedro, M. R.; Seghieri, C.; Nantel, G.; and Brouwer, I. 2007. Dietary diversity score is a useful indicator of micronutrient intake in non-breast-feeding Filipino children. *The Journal of nutrition* 137(2): 472–477.
- Kingma, D. P.; and Ba, J. 2014. Adam: A method for stochastic optimization. *arXiv preprint arXiv:1412.6980*.
- Koppmair, S.; Kassie, M.; and Qaim, M. 2017. Farm production, market access and dietary diversity in Malawi. *Public health nutrition* 20(2): 325–335.
- Muthayya, S.; Rah, J. H.; Sugimoto, J. D.; Roos, F. F.; Kraemer, K.; and Black, R. E. 2013. The global hidden hunger indices and maps: an advocacy tool for action. *PLoS One* 8(6): e67860.
- OpenStreetMap contributors. 2017. Planet dump retrieved from <https://planet.osm.org> . <https://www.openstreetmap.org>.
- Oshri, B.; Hu, A.; Adelson, P.; Chen, X.; Dupas, P.; Weinstein, J.; Burke, M.; Lobell, D.; and Ermon, S. 2018. Infrastructure quality assessment in africa using satellite imagery and deep learning. In *Proceedings of the 24th ACM SIGKDD International Conference on Knowledge Discovery & Data Mining*, 616–625.
- Ronneberger, O.; Fischer, P.; and Brox, T. 2015. U-net: Convolutional networks for biomedical image segmentation. In *International Conference on Medical image computing and computer-assisted intervention*, 234–241. Springer.
- Stefani, A.; Dusfour, I.; Corrêa, A. P. S.; Cruz, M. C.; Dessay, N.; Galardo, A. K.; Galardo, C. D.; Girod, R.; Gomes, M. S.; Gurgel, H.; et al. 2013. Land cover, land use and malaria in the Amazon: a systematic literature review of studies using remotely sensed data. *Malaria journal* 12(1): 1–8.
- UNICEF. 2017. Madagascar Nutrition Investment Case .
- Weiss, D.; Nelson, A.; Gibson, H.; Temperley, W.; Peedell, S.; Lieber, A.; Hancher, M.; Poyart, E.; Belchior, S.; Fullman, N.; et al. 2018. A global map of travel time to cities to assess inequalities in accessibility in 2015. *Nature* 553(7688): 333–336.
- WHO. 2011. *Guideline: vitamin A supplementation in infants and children 6-59 months of age*. World Health Organization.
- Zhang, Z.; Liu, Q.; and Wang, Y. 2018. Road extraction by deep residual u-net. *IEEE Geoscience and Remote Sensing Letters* 15(5): 749–753.